Collisional effects on fast electron generation and transport in fast ignition

H. SAKAGAMI,[1] K. OKADA,[2] Y. KASEDA,[2] T. TAGUCHI,[3] AND T. JOHZAKI[4]

[1]Fundamental Physics Simulation Division, National Institute for Fusion Science, Oroshi-cho, Japan
[2]Department of Physics, Nagoya University, Furo-cho, Chikusa-ku, Nagoya, Japan
[3]Department of Electrical and Electronics Engineering, Setsunan University, Neyagawa, Japan
[4]Institute of Laser Engineering, Osaka University, Suita, Japan

Abstract

As the binary collision process requires much more computation time, a statistical electron-electron collision model based on modified Langevin equation is developed to reduce it. This collision model and a simple electron-ion scattering model are installed into one-dimensional PIC code, and collisional effects on fast electron generation and transport in fast ignition are investigated. In the collisional case, initially thermal electrons are heated up to a few hundred keV due to direct energy transfer by electron-electron collision, and they are also heated up to MeV by Joule heating induced by electron-ion scattering. Thus the number of low energy component of fast electrons increase than that in the collisionless case.

Keywords: Collision model; Cone-guided target; Fast ignition; PIC simulation

1. INTRODUCTION

The FIREX-I project, which is promoted at Osaka University, aims to demonstrate that the imploded core could be heated up to high temperature, 5 keV (Azechi, *et al.*, 2008). Efficient heating mechanisms and achievement of such high temperature have not been, however, clarified yet, and we have been promoting the fast ignition integrated interconnecting code (FI³) project to boldly explore fast ignition frontiers (Sakagami & Mima, 2004; Nakamura *et al.*, 2006, 2008; Sakagami *et al.*, 2006, 2009; Johzaki *et al.*, 2007, 2010). Under this project, interaction between ultrahigh-intense laser and Au cone plasma is computed by PIC code. As the Au plasma is extremely overdense, collisional effects (drag and scattering) within the cone would be important. According to one-dimensional (1D) collisional PIC code PICLS1d (Sentoku & Kemp, 2008), relatively low energy fast electrons, which are expected to mainly heat the core, suffer from strong scattering by highly ionized ions, and lose their kinetic energies through collisional interactions with background electrons and a resistive field. In addition, the return current carried by background electrons is

significantly damped by the increased resistivity (Johzaki *et al.*, 2009).

We have investigated collisional effects on fast electron generation and transport in fast ignition using 1D PIC code with a statistical electron-electron collision model and a simple electron-ion scattering model. In the electron-electron collisional case, initially thermal electrons (<10 keV) are heated up to a few hundred keV due to direct energy transfer from fast electrons to background electrons. Even no energy transfer occurs in electron-ion scattering, background electrons are heated up to MeV by Joule heating which is caused by large resistivity induced by electron-ion scattering.

2. STATISTICAL COLLISION MODEL

2.1. Antonsen's Method

The PIC code introduces a spatial mesh on which fields are defined and the field value on a particle is determined by interpolating field values on neighboring mesh points. This algorithm can greatly reduce calculations, but forces of direct interaction between two particles, i.e., collisions, are automatically filtered out. So PIC codes are widely used for modeling plasmas where collisions are not important in physical processes. When the plasma density is as high as solid density, binary collisions cannot be ignored in

---

determining physical processes such as heat conduction and energy relaxation. Collisional effects can be calculated by the binary collision process, where the collision frequency depends on the relative velocity of pairing particles. Installing the binary collision model into the PIC code, however, requires very long computation time. Thus, many statistical collision models that are based on Langevin equation for electron-electron collisions are already developed to reduce computations (Jones *et al.*, 1996; Manheimer *et al.*, 1997; Cohen *et al.*, 2006). In this work, we use the collision model based on Antonsen's method (Taguchi *et al.*, 2010), which is given by

$$\frac{d\mathrm{v}}{dt} = -(\nu_S + \nu_D)\mathrm{v} + R(t). \tag{1}$$

In our model, the velocity change of each electron by collisions is computed with two components. First one describes a slowing down term with the electron-electron slowing down rate ν_S by Coulomb collisions and an additional term ν_D given by

$$\nu_s = \frac{8\pi e^4 n_e \ln \Lambda}{m_e^2 \mathrm{v}^3}\mu(x), \ \ \mu(x) = \frac{2}{\sqrt{\pi}}\int_0^x e^{-\xi}\sqrt{\xi}d\xi, \ x = \frac{m_e\mathrm{v}^2}{2k_BT_e}, \tag{2}$$

and

$$\nu_D = -\frac{k_BT_e}{m_e\mathrm{v}}\frac{\partial \nu_s}{\partial \mathrm{v}}. \tag{3}$$

Second component represents a fluctuation term, which is calculated as a random force $R(t)$ and $R(t)$ satisfies following equations:

$$\begin{cases} \langle R(t) \rangle = 0 \\ \langle R(t)R(t') \rangle = 2D\delta(t-t') \end{cases}, D = \frac{k_BT_e}{m_e}\nu_s. \tag{4}$$

Once we define T_e as a target state, we can compute time evolution of velocity of electrons, and a velocity distribution function is relaxed to Maxwellian distribution with T_e regardless of initial distributions. Existence of ν_D enables us to correctly compute this relaxation process even for 1D velocity space. These computations have the order of number of particles and computation time can be saved.

In the fast ignition scheme, fast electrons are generated by ultrahigh-intense laser and propagate toward the core through the dense plasma. Thus, collisions between fast (beam) and background electrons should be important. First, we calculate collisional effects between background 90,000 electrons ($\mathrm{v}_{\text{thermal}} = \mathrm{v}_{\text{th0}}$, $\mathrm{v}_{\text{drift}} = 0$) and beam 10,000 electrons ($\mathrm{v}_{\text{thermal}} = 0$, $\mathrm{v}_{\text{drift}} = 5\mathrm{v}_{\text{th0}}$) using Eqs. (1)–(4). The velocity is normalized as $\mathrm{v}/\mathrm{v}_{\text{th0}}$ and ν_S is defined with

$$\nu_s\Delta t = 0.1\frac{\mu(\hat{x})}{\hat{\mathrm{v}}^3}, \ \ \hat{x} = \frac{\hat{\mathrm{v}}^2}{2\hat{\mathrm{v}}_{\text{te}}^2}, \ \hat{\mathrm{v}}_{\text{te}} = \frac{\sqrt{k_BT_e/m_e}}{\mathrm{v}_{\text{th0}}}. \tag{5}$$

where Δt is the size of a time step of time-differentiated Eq. (1) and v_{th0} is an initial thermal velocity. From Eqs. (3) and (5), ν_D is defined with

$$\nu_D\Delta t = 0.1\left[\frac{3\hat{\mathrm{v}}_{\text{te}}^2}{\hat{\mathrm{v}}^5} - \frac{1}{\hat{\mathrm{v}}^3}\frac{\partial}{\partial \hat{x}}\right]\mu(\hat{x}). \tag{6}$$

The normalized random force $R(t)$ can be calculated from normalized D, which is defined with

$$\hat{D} = \hat{\mathrm{v}}_{\text{te}}^2\nu_S\Delta t. \tag{7}$$

In this normalized calculation, time scale is independent from plasma parameters and relaxation time is characterized by time step. Our statistical collision model is extended to Maxwellian distribution with the drift velocity, and the thermal and drift velocities of the target state are determined as an equilibrium state to conserve total energy and momentum of electrons. Time evolutions of electron velocity distribution function and time evolutions of thermal and drift velocities of all electrons are shown in Figure 1a and 1b, respectively. All electrons are relaxed to one temperature Maxwellian distribution as the thermal equilibrium state, and each velocity is relaxed to the desired value of the equilibrium state, namely $1.79\mathrm{v}_{\text{th0}}$ and $0.5\mathrm{v}_{\text{th0}}$, respectively. Time evolutions of background, beam, and total electron energies are shown in Figure 1c. The total energy is not conserved in early stage. In this situation, beam and background electrons are independently relaxed to the target (equilibrium) state, where the total energy and momentum of electrons are the same as those of the initial state. As the mean velocity of background electrons is lower than that of beam electrons, background electrons are relaxed much faster than beam electrons because ν_S is inversely proportional to the cube of electron velocity. Thus the background electron energy quickly increases, but the beam electron energy slowly decreases without conserving the total energy.

2.2. Improved Collision Model

To conserve the total energy and momentum of electrons at any time, we improve algorithm of our statistical collision model as follows: (1) discriminate between background and beam electrons, (2) measure thermal and drift velocities of background electrons as the target state, (3) compute collisions of beam electrons with the target state and calculate momentum and energy losses, (4) compute collisions of background electrons with the target state, and (5) correct background electron velocity to conserve the total energy and momentum (Manheimer *et al.*, 1997), Momentum and energy losses are given by

$$\sum_{beam}(m_e\mathrm{v}_{\text{before}} - m_e\mathrm{v}_{\text{after}}) = \Delta M,$$

$$\sum_{beam}\left(\frac{1}{2}m_e\mathrm{v}_{\text{before}}^2 - \frac{1}{2}m_e\mathrm{v}_{\text{after}}^2\right) = \Delta E. \tag{8}$$
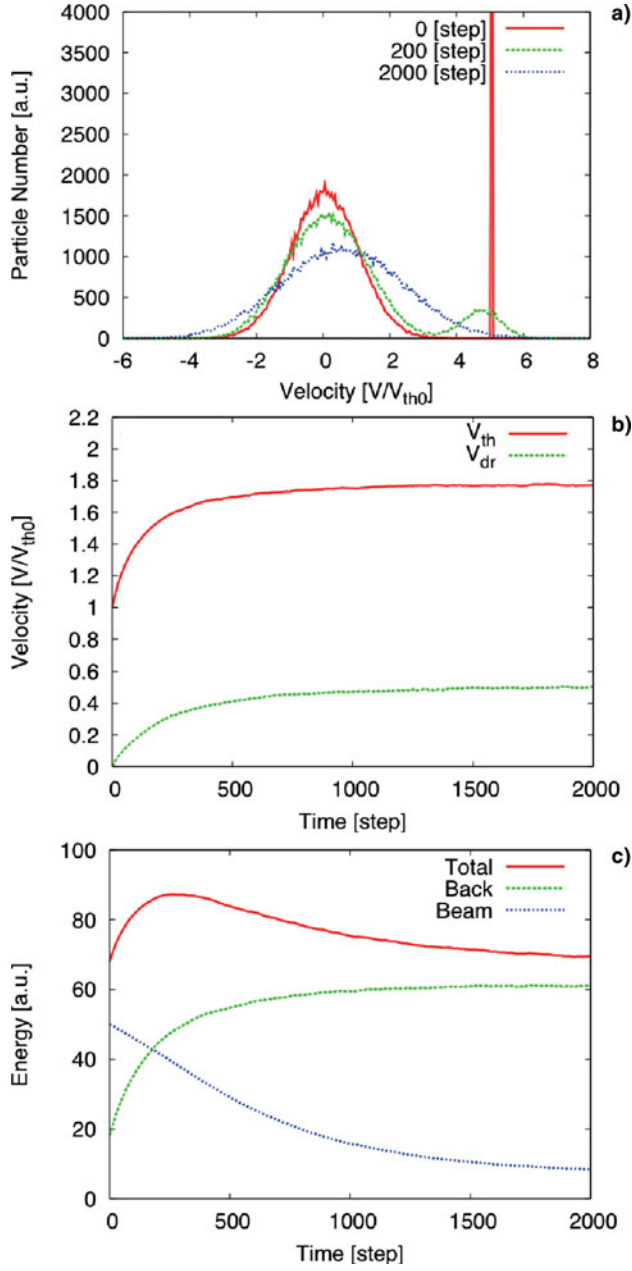
Fig. 1. (Color online) Collisions between background and beam electrons. Time evolutions of (**a**) electron velocity distribution function, (**b**) thermal (red) and drift (green) velocities of all electrons, and (**c**) background (green), beam (blue) and total (red) electron energies. In figure (a), colors of red, green and blue indicate time step 0, 200, and 2000, respectively.

We define correction terms for background electrons as follows:

$$v'_{\text{after}} = \alpha(v_{\text{after}} - v_{\text{drift}}) + v_{\text{drift}} + \beta. \quad (9)$$

The conservation of the total momentum and energy after correction is given by

$$\sum_{background} (m_e v'_{\text{after}} - m_e v_{\text{before}}) = \Delta M,$$

$$\sum_{background} \left(\frac{1}{2} m_e v'^2_{\text{after}} - \frac{1}{2} m_e v^2_{\text{before}}\right) = \Delta E. \quad (10)$$

As the thermal and drift velocities of background electrons are the same as those of the target state, we can assume that collision calculations for background electrons preserve the total momentum and energy and give following equations:

$$\sum_{background} (m_e v_{\text{after}} - m_e v_{\text{before}}) = 0,$$

$$\sum_{background} \left(\frac{1}{2} m_e v^2_{\text{after}} - \frac{1}{2} m_e v^2_{\text{before}}\right) = 0. \quad (11)$$

From Eqs. (8)–(11), we can derive the correction terms as follows:

$$\alpha = \sqrt{\frac{\frac{2\Delta E}{m_e} - \frac{\Delta M^2}{N m_e^2} - \frac{2 v_{\text{drift}} \Delta M}{m_e}}{\sum_{background} v^2_{\text{after}} - N v^2_{\text{drift}}} + 1}, \quad \beta = \frac{\Delta M}{N m_e}, \quad (12)$$

where N is the number of background electrons.

Time evolutions of electron velocity distribution function and time evolutions of thermal and drift velocities of all electrons for the same problem are shown in Figure 2a and 2b, respectively. We give the target state as the equilibrium state in the previous collision model, but each velocity is asymptotically approaching to the value of the equilibrium state even though we give only the current state as the instantaneous target state of background electrons. Time evolutions of background, beam, and total electron energies are shown in Figure 2c. The total energy is always conserved as we expect. It is noted that the beam electron energy exponentially drops in Figure 1c, but it has an inflection point in Figure 2c just as observed in the binary collision calculation (Sentoku & Kemp, 2008).

We extend our electron-electron collision model to a two-dimensional velocity space, and then install it into 1D PIC code. As electron does not lose its momentum and only changes its direction by the electron-ion collision because of large mass difference, we also install a simple electron-ion scattering as the electron-ion collision model in addition to the electron-electron collision model. In this scattering model, the scattering angle of electrons is randomly chosen with the Gaussian distribution as described below (Takizuka & Abe, 1977):

$$\begin{cases} \langle \Delta \Theta \rangle = 0 \\ \left\langle \tan^2\left(\frac{\Delta \Theta}{2}\right) \right\rangle = v_{ei} \Delta t \end{cases}, \quad v_{ei} = \frac{4\pi e^4 Z^2 n_i \ln \Lambda}{m_e^2 v^3} \mu(x), \quad (13)$$
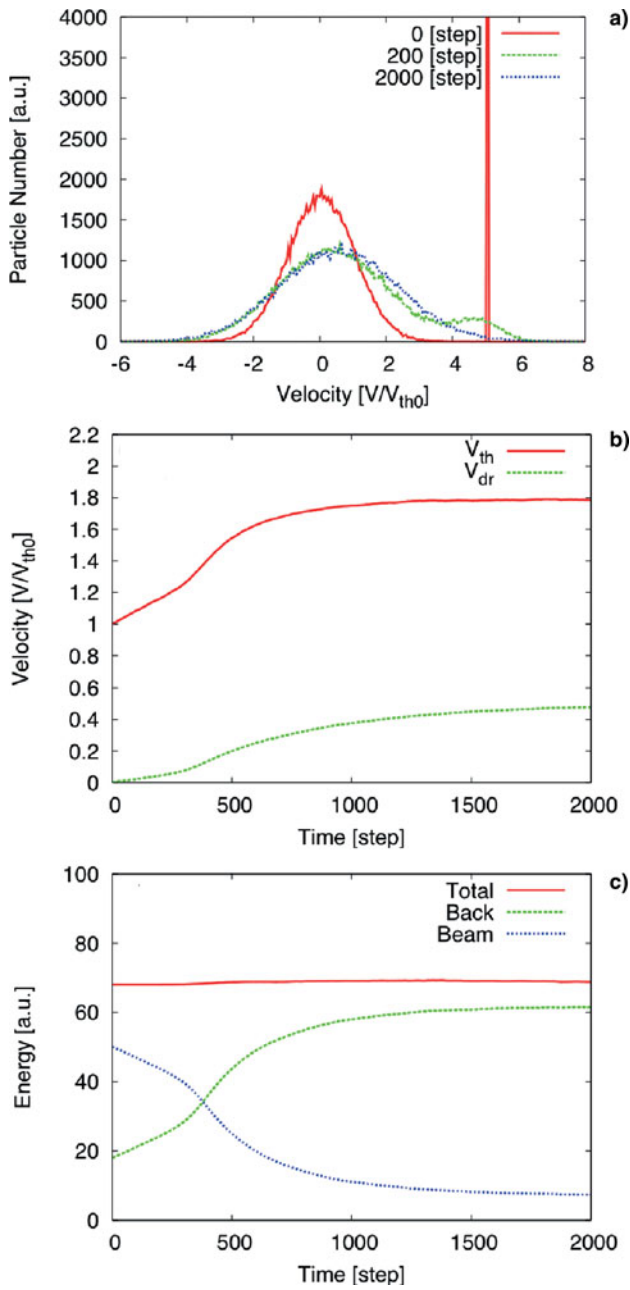
Fig. 2. (Color online) Collision calculations with improved model. Time evolutions of (**a**) electron velocity distribution function, (**b**) thermal (red) and drift (green) velocities of all electrons, and (**c**) background (green), beam (blue) and total (red) electron energies. In figure (a), colors of red, green and blue indicate time step 0, 200, and 2000, respectively.

Fig. 3. (Color online) Collisional effects. (**a**) Time evolutions of fast electron beam intensities, (**b**) time averaged fast electron energy spectra, and (**c**) an enlarged low energy part (< 2 MeV) of figure (b). In all figures, colors of blue, red and green indicate without collisions, with the electron-electron collision model and with the electron-ion scattering model, respectively.

where $\Delta\Theta$ is a scattering angle and Z is ionization degree of ions. We divide the whole simulation system into subspaces. In each subspace, the target state is individually evaluated and collision calculations are performed.

3. COLLISIONAL EFFECTS

To evaluate collisional effects in the fast ignition, we set the heating laser, which is injected from the left boundary, to
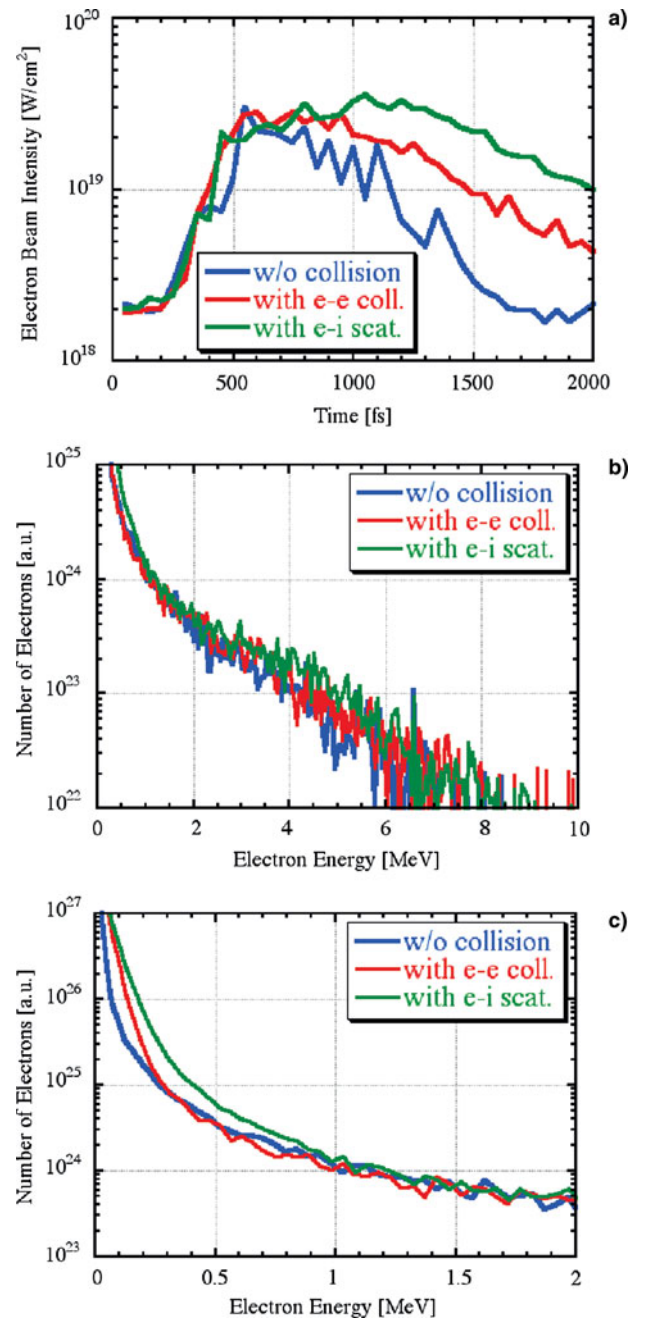
$\lambda_L = 1.06$ μm, $\tau_{rise}/_{fall} = 200$ fs, $\tau_{flat} = 500$ fs, $I_L = 10^{20}$ W/cm^2, and the gold-cone tip is introduced as 10 μm, $500 n_{cr}$, real mass and $Z = 30$ plasma with preformed gold plasma, which has a exponential profile of the scale length $L = 1$ μm with density from $0.1 n_{cr}$ up to $500 n_{cr}$. A fast electron beam is observed at 6 μm from the right boundary. To ignore a circulation of fast electrons that are reflected by

the sheath field at the right edge of the plasma, we introduce an artificial cooling region at 1 to 5 μm from the right boundary, in which fast electrons are gradually cooled down to the initial temperature. To enhance the collisional effects, we set the Coulomb logarithm for both electron-electron and electron-ion collisions to 100, which is roughly equivalent to the value in $2000n_{cr}$ plasmas. Time evolutions of fast electron beam intensity, time averaged fast electron energy spectra for the cases without collisions, with only electron-electron collision and with only electron-ion scattering are shown in Figure 3a and 3b, respectively. A low energy part (<2 MeV) in Figure 3b is enlarged in Figure 3c. The fast electron beam intensity is enhanced by electron-electron collisional effects after 800 fs, and more by electron-ion scattering. Fast electron energy spectra are similar for all cases, but the number of sub-MeV electrons is also enhanced by collisional effects (see Fig. 3c) and these increments result in rises of the beam intensity. As energy of fast electrons can be directly transferred to background electrons in the electron-electron collision, initially thermal electrons (<10 keV) can receive the energy from fast electrons and are heated up to a few hundred keV. On the other hand, no energy transfer, however, occurs with the electron-ion scattering. The return current carried by background electrons is driven by the fast electron current to maintain current neutrality. The mean flow velocity of background electrons is much slower than that of fast electrons, because the number of background electrons is much more than that of fast electrons. As the electron-ion collision frequency is inversely proportional to the cube of the electron velocity, the background electron flow is much disturbed by the electron-ion scattering and cannot cancel the fast electron flow. Thus the electrostatic field is induced to preserve the current neutrality. This electrostatic field and the return current can cause Joule heating. As the Joule heating rate is proportional to $j \cdot E$, we plot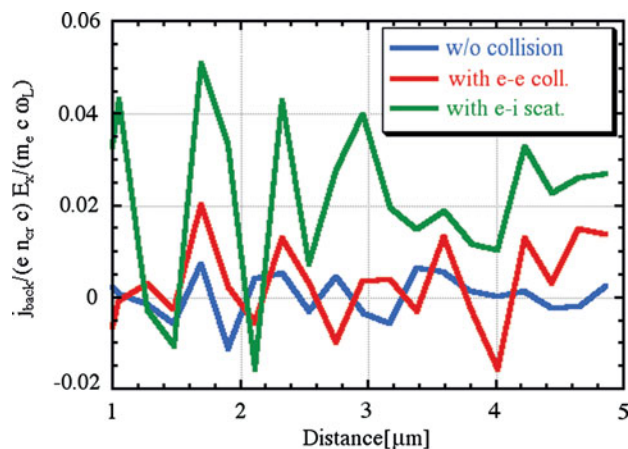 the product of the electrostatic field and the return current carried by background electrons behind the laser front ($500n_{cr}$ gold-cone tip plasmas are initially located from 0 to 10 μm) at 1 ps for the cases without collisions, with only electron-electron collision and with only electron-ion scattering in Figure 4. It is confirmed that the Joule heating rate for the case of electron-ion scattering is much higher than the other cases, and background electrons are heated up to MeV by Joule heating induced by the electron-ion scattering.

It is noted that computation time with the electron-electron collision model is 58% longer than that without the collision model and 38% with the electron-ion scattering model. For the parameters used here, collisions have not significant effects. It is also ambiguous that increment of electrons in low energy by collisions has the effect on efficient core heating. More research is needed to investigate collisional effects on fast electron generation and transport in fast ignition.

REFERENCES

AZECHI, H. & FIREX PROJECT (2008). The FIREX program on the way to inertial fusion energy. *J. Phys. Conf. Ser.* **112**, 012002.

COHEN, B.I., DIVOL, L., LANGDON, A.B. & WILLIAMS, E.A. (2006). Effects of ion-ion collisions and inhomogeneity in two-dimensional kinetic ion simulations of stimulated Brillouin backscattering. *Phys. Plasmas* **13**, 022705.

JOHZAKI, T., SAKAGAMI, H., NAGATOMO, H. & MIMA, K. (2007). Holistic simulation for FIREX project with FI[3]. *Laser Part. Beams* **25**, 621–629.

JOHZAKI, T., SENTOKU, Y., NAGATOMO, H., SAKAGAMI, H., NAKAO, Y. & MIMA, K. (2009). Core heating properties in FIREX-I — Influence of cone tip. *Plasma Phys. Contr. Fusion* **51**, 014002.

JOHZAKI, T., NAGATOMO, H., SUNAHARA, A., CAI, H.B., SAKAGAMI, H. & MIMA, K. (2010). Integrated simulations of core heating in cone-guiding fast ignition FIREX-I. *J. Phys. Conf. Ser.* **244**, 022040.

JONES, M.E., LEMONS, D.S., MASON, R.J., THOMAS, V.A., WINSKE, D. (1996). A grid-based Coulomb collision model for PIC Codes. *J. Comput. Phys.* **123**, 169–181.

MANHEIMER, W.M., LAMPE, M. & JOYCE, G. (1997). Langevin representation of Coulomb collisions in PIC simulations. *J. Comput. Phys.* **138**, 563–584.

NAKAMURA, T., SAKAGAMI, H., JOHZAKI, T., NAGATOMO, H. & MIMA, K. (2006). Generation and transport of fast electrons inside cone targets irradiated by intense laser pulses. *Laser Part. Beams* **24**, 5–8.

NAKAMURA, T., MIMA, K., SAKAGAMI, H., JOHZAKI, T. & NAGATOMO, H. (2008). Generation and confinement of high energy by irradiation of ultra-intense short laser pulses onto cone targets. *Laser Part. Beams* **26**, 207–212.

SAKAGAMI, H. & MIMA, K. (2004). Interconnection between hydro and PIC codes for fast ignition simulations. *Laser Part. Beams* **22**, 41–44.

Fig. 4. (Color online) Spatial profiles of the Joule heating rate behind the laser front. Colors of blue, red and green indicate without collisions, with the electron-electron collision model and with the electron-ion scattering model, respectively.

SAKAGAMI, H., JOHZAKI, T., NAGATOMO, H. & MIMA, K. (2006). Fast ignition integrated interconnecting code project for cone-guided targets. *Laser and Part. Beams* **24**, 191–198.

SAKAGAMI, H., JOHZAKI, T., NAGATOMO, H. & MIMA, K. (2009). Generation control of fast electron beam by low density foam for FIREX-I. *Nucl. Fusion* **49**, 075026.

SENTOKU, Y. & KEMP, A.J. (2008). Numerical methods for particle simulations at extreme densities and temperatures: Weighted particles, relativistic collisions and reduced currents. *J. Comput. Phys.* **227**, 6846–6861.

TAGUCHI, T., ANTONSEN JR., T.M., PALASTRO, J., MILCHBERG, H. & MIMA, K. (2010). Particle in cell analysis of a laser-cluster interaction including collision and ionization processes. *Opt. Expr.* **18**, 2389–2405.

TAKIZUKA, T. & ABE, H. (1977). A binary collision model for plasma simulation with a particle code. *J. Comp. Phys.* **25**, 205–219.